Maria E. Zamiralova

MSc, PhD candidate
Delft University of Technology
Faculty of Mechanical, Maritime and
Materials Engineering

Gabriel Lodewijks

Professor of Transport Engineering and
Logistics
Delft University of Technology
Faculty of Mechanical, Maritime and
Materials Engineering

Energy Consumption of Pipe Belt Conveyors: Indentation Rolling Resistance

This paper presents a detailed approach for the calculation of the indentation rolling resistance forces of pipe belt conveyors. The viscoelastic behaviour of the belt's rubber is modelled as a three-dimensional generalized model with multiple Maxwell parameters incorporated with a Winkler foundation. The step by step calculation of the indentation rolling resistance factor is provided in this paper. Attention is also paid to the determination of the normal contact forces as concentrated load forces, exerted on each roll of an idler set. Load forces depend on the mass of the transported material, the filling ratio of the pipe, and the mass and stiffness of the belt.

Keywords: *pipe belt conveyor, belt conveyor, rolling contact, rolling friction, indentation rolling resistance, viscoelasticity.*

1. INTRODUCTION

Tubular pipe conveyors are becoming more and more popular in the bulk material handling industry. For example, they are applied when the installation of a belt conveyor is required in difficult topographical conditions, rough weather conditions, and for the transportation of dusty, contaminated, and toxic materials. The main advantages of using a pipe conveyor, instead of a conventional open trough belt conveyor, are the ability to have a completely enclosed transport system design, and its geometrical flexibility.

The high demand for pipe conveyor installations justifies research into the power consumption of pipe conveyors that significantly depend on rolling resistance forces. The total rolling resistance force, which is distributed over each roll of the idler set, is the sum of the resistance forces due to the rotational inertia of the idlers, the flexural deformation of the material and the belt, and the indentation rolling resistance due to the indentation of the idler rolls into the belt. The indentation rolling resistance of pipe belt conveyors is higher than the indentation rolling resistance of conventional open trough belt conveyors. In case of the latter, it may already form up to 61% of the total rolling resistance [1].

Various researchers have developed models that describe the indentation rolling resistance for flat-belt, conventional open trough and even pouch belt conveyors.

Preliminary values for the dimensionless indentation rolling resistance factor for pipe belt conveyors were presented by Dmitriev and Sergeeva in [2], used Jonkers indentation model [3] as a basic.

As it is shown in [4], this approach comprises assumptions, which causes substantial errors in the results of the indentation rolling resistance and needs to be reconsidered (see paragraph 3.1).

Therefore, in order to obtain more accurate results for the calculation of the indentation rolling resistance factor of pipe belt conveyors, a three-dimensional contact model with multiple Maxwell parameters is presented in this paper. The presented model provides a calculation method for obtaining the normal contact forces, and takes in account geometrical specificity of the pipe conveyor design.

2. LOAD FORCES CALCULATION

The indentation rolling resistance factor is governed by the normal contact forces, and is equivalent to the concentrated load forces that are exerted on the rolls of a hexagonal 6-roll idler set. The load force for each roll is comprised of forces from the material and the belt. Those forces depend on the weight of the transported material, the filling ratio of the pipe cross section, and the weight and stiffness of the belt.

2.1 Load forces from the material

The nature of the material load distribution, when the loaded conveyor is in motion, is generally defined by the active/passive pressure theory of the material's behaviour.

When the belt passes through the idler assembly, the belt is in unfolding opening out process. During this time period, the loaded material causes a distributed active pressure on the belt surface, due to the weight of the material. The active material pressure is exerted solely along half of the conveyor pitch *l'* (see Fig. 1). The next half of the carry spacing before the belt passes next idler assembly, the belt compresses the material, which in turn reasons passive material pressure.
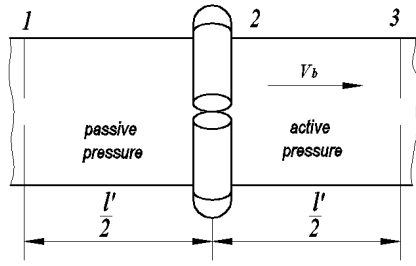
Figure 1. Passive and active material load pressure distribution [2]

The distributed active $p_{act}(\varphi, \alpha)$ [Pa] and passive pressure $p_{pas}(\varphi, \alpha)$ [Pa] from the loaded material, with density ρ [kg/m^3], along the width of the belt, which is folded in a pipe with radius R_p [m], can be described with the following equations, also see Figure 2. These equations were developed by Gushin [5] for deep trough belt conveyors, but can also be used for pipe conveyor calculations:

$$p_{act}(\varphi, \alpha) = R_p \cdot \rho \cdot g \int C_{act}(\alpha) d\alpha , \qquad (1)$$

$$p_{pas}(\varphi, \alpha) = R_p \cdot \rho \cdot g \int C_{pas}(\alpha) d\alpha , \qquad (2)$$

where functions $C_{act}(\alpha)$ and $C_{pas}(\alpha)$ equals:

$$C_{act}(\alpha) = (\cos 2\varphi + \cos \alpha) \cdot (\cos^2 \alpha + m \cdot \sin^2 \alpha), \quad (3)$$

$$C_{pas}(\alpha) = (\cos 2\varphi + \cos \alpha) \cdot (\cos^2 \alpha + \frac{\sin^2 \alpha}{m}). \quad (4)$$

In these equations, the m - coefficient of the material mobility motion, is expressed by the angle of the internal friction of the bulk material; φ - angle, identifying the filling ratio of the cross section; α - angle of deviation; θ – the angle of repose of the bulk material in motion (see Fig. 2).
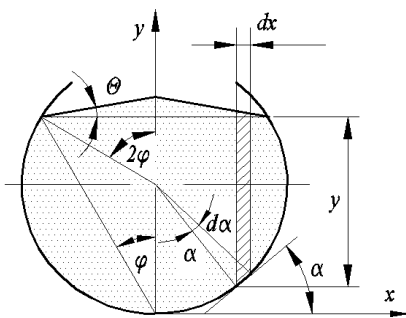

Figure 2. Cross section of the deep trough belt conveyor [5]

As the active and passive material load pressures are exerted along half of the conveyor pitch, the linear distributed load $P(\varphi, \alpha)$ [N/m], from the material can be found as follows:

$$P(\varphi, \alpha) = \frac{l'}{2}(p_{act} + p_{pas}). \qquad (5)$$

The equivalent concentrated load $F_{mn}(\alpha, \Delta\alpha)$ [N] for the length $R_p \cdot \Delta\alpha$ along the belt width equals:

$$F_{mn}(\alpha, \Delta\alpha) = R_p^2 \cdot \Delta\alpha \cdot \rho \cdot g \cdot \frac{l'}{2} \times$$

$$\times \left(\int_\alpha^{\alpha+\Delta\alpha} C_{act}(\alpha) d\alpha + \int_\alpha^{\alpha+\Delta\alpha} C_{pas}(\alpha) d\alpha \right). \qquad (6)$$

Eventually, the concentrated forces due to the material load distribution for each roll of the idler set, can be obtained from (6) by integrating with appropriate limits, from the interval from 0 to $\pi - 2\varphi$ in respect of the superposition principle. For instance, for $\varphi = \frac{\pi}{12}$ the forces, denoted as shown in Fig. 3, can be determined as follows:

$$F_{m1} = 2\frac{\pi}{6} R_p^2 \cdot \rho g \frac{l'}{2} \int_0^{\pi/6} \left(C_{pas}(\alpha) + C_{act}(\alpha) \right) d\alpha , \quad (7)$$

$$F_{m2} = F_{m6} = \frac{\pi}{3} R_p^2 \rho g \frac{l'}{2} \int_{\pi/6}^{\pi/2} \left(C_{act}(\alpha) + C_{pas}(\alpha) \right) d\alpha , \quad (8)$$

$$F_{m3} = F_{m5} = \frac{\pi}{3} R_p^2 \rho g \frac{l'}{2} \int_{\pi/2}^{5\pi/6} \left(C_{act}(\alpha) + C_{pas}(\alpha) \right) d\alpha . \quad (9)$$
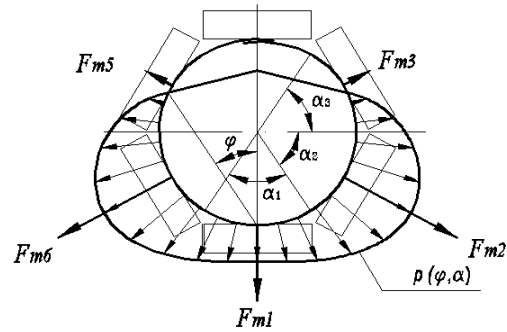

Figure 3. Material load distribution in cross section of the pipe conveyor [2].

2.2 Load forces from the belt

The load from the belt is the result of the weight and stiffness of the belt material. The concentrated force F_{bn} [N] from the belt with line mass per unit of length m'_b [kg/m] and width B [m] for each roll of the idler assembly is evaluated by follows:

$$F_{b1} = F_{stif} + \frac{m'_b g}{B} \cdot \frac{2\pi R_p}{6} \cdot l' , \qquad (10)$$

$$F_{b2} = F_{b6} = F_{stif} + \frac{m'_b g}{B} \cdot \frac{2\pi R_p}{6} \cdot l' \cos \frac{\pi}{3} , \qquad (11)$$

$$F_{b3} = F_{b5} = F_{stif} - \frac{m'_b g}{B} \cdot \frac{2\pi R_p}{6} \cdot l' \cos \frac{\pi}{3} , \qquad (12)$$

$$F_{b4} = F_{stif} - \frac{m'_b g}{B} \cdot \frac{2\pi R_p}{6} \cdot l' . \qquad (13)$$

The expansion force F_{stif} [N] represents the stress state of the belt, which is folded from a flat shape into a pipe. This force is caused by the stiffness of the belt

material. This force can be calculated as it is recommended by Chernenko in [6], which was derived by considering the belt as an orthotropic shell that is bent into a cylindrical shape.

$$F_{stif} = \frac{E_{b2}}{1 - \mu_1 \mu_2} \cdot \frac{\alpha h_b^3}{24 R_p^2} \cdot l'. \qquad (14)$$

Here E_{b2} [Pa] – Young's modulus of the belt in lateral direction; μ_1, μ_2 - Poisson ratios in longitudinal and lateral direction respectively; h_b [m] – thickness of the belt; $\alpha = \frac{\pi}{3}$ - angle of the rolls installation relatively to each other.

Eventually, the total normal contact force for each roll F_n [N] for each n-th roll is formed by the sum of forces from the material and the belt:

$$F_n = F_{mn} + F_{bn}. \qquad (15)$$

3. THE INDENTATION ROLLING RESISTANCE

The indentation rolling resistance force arises when the belt is in motion over the idler rolls under the compression load. It is caused by the viscoelastic properties of the belt rubber cover. After the deformation the viscoelastic rubber that covers the belt's carcass does not have enough time to completely recover back into its initial state. This phenomenon causes an asymmetric stress distribution between the rolls and the belt.

In order to evaluate the indentation rolling resistance and obtain accurate results, it is important to choose the correct model. The chosen model should be computationally friendly and should give an appropriate level of accuracy.

3.1 Overview and choice of the model

A significant amount of research that describes the indentation rolling resistance has been published recently. Two of the most commonly used indentation models were developed by Jonkers [3] and Spaans [7] for the calculation of the indentation rolling resistance. Researchers prescribe the indentation force in terms of the vertical load, instead of the geometrical indentation depth. Both approaches use a 3 parameter Maxwell model, and assume that the indentation strain profile is symmetrical with respect to the centre line of the idler and that it does not depend on the belt speed. As shown in [4], these assumptions are not acceptable and lead to the overestimation of the total indentation resistance force. May et al. [8] also presented a model for the calculation of the indentation rolling resistance forces by using a 3 parameter Maxwell model (so-called SLS – standard linear solid) with a single relaxation time. For simplification the so-called Winkler viscoelastic string "matrass" foundation is used. Hunter uses a half space plane approach in the description of his indentation model [9]. This allowed for the inclusion of the creep-response viscoelastic behaviour.

Lodewijks [4] developed an approach similar to May, and added the friction correction factor. This factor takes into account Hunter's model with the shear stress between adjusted Winkler foundation strings. Rudolphi and Reicks [10] used a one-dimensional model with an expanded generalized Maxwell solid model. However, as noted by Lodewijks [4], a three parameter Maxwell model, with a single relaxation time, provides a simple and sufficient description of the contact phenomena between the idler rolls and a flat belt.

In case of a pipe belt conveyor, the curved contact surfaces of the belt and idler rolls have an effect on the indentation phenomena. The contact area between a pipe belt and a roll has an elliptical shape. Figure 4 illustrates the idler roll as a rigid cylinder with radius R_1, rolling over the curved viscoelastic surface of the belt with radius R_2. The geometry of the contact spot indicates, that the contact time depends on the contact width along the length of the idler roll. This makes the application of a 3 parameter (two springs and one dashpot) Maxwell model with one single relaxation time insufficient. Therefore a three-dimensional contact model with a generalized Maxwell model is used. This model was developed by Nutall and Lodewijks [11] for the pouch belt conveyor system and has been adapted here for the pipe conveyor system. The indentation depth of the model is described in terms of the normal force on the idler rolls.
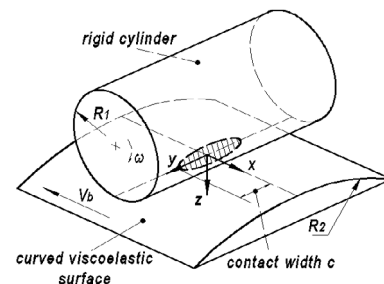

Figure 4. Cylinder rolling over a curved surface [11]

3.2 Indentation contact model

The calculation model, which describes the indentation contact problem, is distributed as illustrated in Figure 5. The belt moves with a linear speed V_b [m/s], and is covered with a viscoelastic layer with a thickness h [m]. In the case of pipe belt conveyors, thickness h equals thickness of the rubber ply belt bottom cover. A rigid roll with a radius R_1 [m], is compressed under the contact load F_z [N], and rolls over the belt cover with an angular frequency w [s^{-1}], and causes the reaction normal force F_N [N]. The cylinder indents into the viscoelastic base with a depth of z_0 [m]. The first point, where the rubber and the roll come into the physical contact, is specified as $x = a$; at the point $x = -b$ the physical contact between surfaces ends.

As was derived in [11], the deformation of the contact viscoelastic plane with Winkler foundation in 3 dimensions, can be described by (16) as follows:

$$w(x, y) = z_0 - \frac{x^2}{2R_1} - \frac{y^2}{2R_2}, \qquad (16)$$

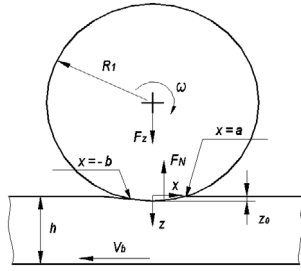where $-b \leq x \leq a$ and $x \ll R_1$, $y \ll R_2$.

Figure 5. Indentation calculation model [11].

The pressure distribution in the contact plane can be expressed as:

$$\sigma(x, y) = \frac{E_0}{2R_1 h}(a^2 - x^2) + \sum_{i=1}^{m} \frac{E_i k_i}{hR_1} \times$$

$$\times \left(x - a + (a + k_i)\left(1 - \exp\left(\frac{x-a}{k_i}\right)\right)\right) \qquad (17)$$

In (17) parameter $k_i = \frac{\eta_i V_b}{E_i}$ $[m^4/s^2]$; E_0 [Pa]

E_i [Pa] - springs stiffness and η_i [Nm/s] - damping factor of the Maxwell parameters of the generalized spring-dashpot assembly (see Figure 6).
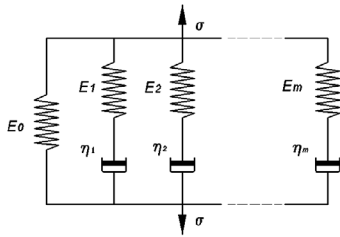

Figure 6. Generalized Maxwell model with *m* elements

The normal contact force on each idler roll determines the appropriate indentation depth and satisfies (18), which was obtained by integrating the contact plane pressure distribution over the whole contact area:

$$F_z = 2\int_0^c \int_{-b(y)}^{a(y)} \sigma(x, y)\,\mathrm{d}x\,\mathrm{d}y. \qquad (18)$$

In the presented formula limit under the integral sign - function $-b(y)$ can be found by setting $\sigma(-b(y), y) = 0$, and cannot be presented in explicit form. In order to avoid this, the contact plane is divided into strips, in order to simplify the integration process of the stress distribution over the entire contact region.

The step by step calculation of the indentation rolling resistance and indentation rolling resistance factor will be described in the next paragraph.

3.3 Calculation method

1) The calculation of the normal contact force for each roll of the idler set F_n, as described in paragraph 2. The initial guess value for the indentation depth z_0 should be set on the interval $0 < z_0 < h$.

2) The half-length c [m] of the contact region (see Figure 4) can be determined by setting the stress distribution $\sigma(0, c) = 0$. Therefore

$$z_0 = \frac{c^2}{2R_2} \Rightarrow c = \sqrt{2R_2 z_0}. \qquad (19)$$

3) The values of the y [m] can be set by dividing the contact region with length $2c$ into strips.

The necessary number of divisions should be determined by optimizing between the calculation time consuming and the desired level of accuracy. As presented in Figure 7, the number of strips was chosen equal to $q=7$. As it stated in [11], this number of elements shows acceptable accuracy.
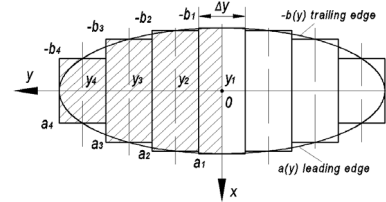

Figure 7. contact region, divided into strips.

After dividing the contact area, the values of the y coordinates of the centrelines of each strip for the half-length equal:

$$y_1 = 0; \quad y_2 = \frac{2c}{q}; \quad \dots; y_p = \frac{6c}{q}. \qquad (20)$$

where $p = \frac{q+1}{2}$ for odd numbers of the q.

4) The calculation of the x-coordinates of the leading edge function $x = a(y)$ for the centrelines of each strip.

Along the edge $x = a(y)$ there is no deformation, so

$$w(a(y), y) = 0 \Rightarrow a(y) = \sqrt{2R_1\left(z_0 - \frac{y^2}{2R_2}\right)}. \qquad (21)$$

According to y_1, y_2, ..., y_p the values of $a(y)$ yield:

$$a_1(y_1) = \sqrt{\frac{R_1(c^2 - y_1^2)}{R_2}}, \qquad (22)$$

$$a_2, a_3, \dots, a_p.$$

5) The calculation of the x-coordinates of the trailing edge is the function $x = -b(y)$ for the centreline of each strip since $\sigma(-b(y), y) = 0$:

$$b_1 \Leftarrow \frac{E_0}{2R_1 h}(a_1^2 - b_1^2) + \sum_{i=1}^{m} \frac{E_i k_i}{hR_1} \times$$

$$\times\left(-b_1 - a_1 + (a_1 + k_i)\left(1 - \exp\left(-\frac{b_1 + a_1}{k_i}\right)\right)\right) = 0, \quad (23)$$

$$b_2, \ b_3, \ \ldots, \ b_p.$$

6) The calculation of the normal contact load for each roll of the idler assembly, from (18).

In order to obtain a result, the integration operation needs to be replaced with a summation operation. For odd number q of strips, (18) can be transformed into (26):

$$F_z^{calc} = 2\left[\frac{\Delta y}{2}\int_{-b_1}^{a_1}\sigma(x,y)\mathrm{d}x + \Delta y\sum_{j=2}^{p}\int_{-b_j}^{a_j}\sigma(x,y)\mathrm{d}x\right], \quad (24)$$

where $\Delta y = \dfrac{2c}{q}$.

7) Validation F_z and determine the correct value of the indentation depth z_0.

The calculated normal contact force F_z^{calc} from (24), is dependent on the indentation depth z_0, and should be equivalent to the concentrated load force $F_z = F_n$, which are obtained from (15) in Paragraph 2, for each roll from the idler set. The correct value of the indentation depth z_0, $0 < z_0 < h$, can be found from following equation:

$$F_z - F_z^{calc}(z_0) = 0. \quad (25)$$

The solution of (25) can be obtained through a numerical method, using a root-finding algorithm. Here the secant method is used for the approximation function $f(z_0) = F_z - F_z^{calc}(z_0)$. The root-searching iteration of z_0 repeats, until the accuracy of the convergence reaches 10^{-4}.

8) Recalculating the correct values of the leading and trailing edges $(-b_1; a_1)$, $(-b_2; a_2)$, ..., $(-b_p; a_p)$ from (21) – (23) based on the correct value z_0, found from the previous step.

9) Calculation resistance force F_{rn}.

The torque M_y [Nm] from the asymmetric pressure distribution about the centre of the roller can be found:

$$M_y = 2\int_{0}^{c}\int_{-b(y)}^{a(y)} x \cdot \sigma(x,y)\mathrm{d}x\mathrm{d}y. \quad (26)$$

Rolling resistance force F_{rn}, for each n-th roll of the idler set depends on the resistance torque:

$$F_{rn} = \frac{M_y}{R_1}. \quad (27)$$

It can be evaluated from (28), replacing integration by a sum operation as follows:

$$F_{rn} = \frac{2}{R_1}\left[\frac{\Delta y}{2}\int_{-b_1}^{a_1} x\sigma(x,y)\mathrm{d}x + \Delta y\sum_{j=2}^{p}\int_{-b_j}^{a_j} x\sigma(x,y)\mathrm{d}x\right] \quad (28)$$

10) Calculation indentation rolling resistance factor f_{ind}.

Eventually the indentation rolling resistance friction factor, which is frequently used for the calculation of the energy consumption of belt conveyors for the pipe conveying systems equals:

$$f_{ind} = \frac{\sum_{n=1}^{6} F_{rn}}{(m'_m + m'_b)gl'}, \quad (29)$$

where m'_m [kg/m] and m'_b [kg/m] - line mass of the material and belt per unit of length respectively.

4. RESULTS

In the previous paragraphs the equations were obtained for the indentation rolling resistance factor and geometrical data for the contact regions for the pipe conveyor. In these simulations the radius of the roll R_1 was set equal 0.0795 m, the radius of the curved surface equalled to the radius of the pipe $R_2 = R_p = 0,2$ m. For the belt with width $B = 1,6$ m and thickness $h_b = 0,012$ m, the thickness of the rubber ply belt bottom cover was chosen $h = 0,002$ m. Young's modulus of the belt in lateral direction E_{b2} was assumed equal $6,464 \cdot 10^7$ Pa; Poisson ratios in longitudinal and lateral directions - $\mu_1 = 0,45$, $\mu_2 = 0,15$ - respectively; density of the transported material - $\rho = 1500 \ kg/m^3$. In the presented simulations the number of strips was chosen equal to $q=7$. The number of the Maxwell parameters was restricted to 3. The values of the elements were validated to the viscoelastic rubber test data in [4] and equal: $E_0 = 7 \cdot 10^6 \ Nm^{-2}$; $E_1 = 2,5 \cdot 10^8 \ Nm^{-2}$; $\eta_1 = 1875 \ Nm^{-2}s$.

Figure 8 shows the results for the rolling friction coefficient f_{ind} for the 25%, 50% and 75% filling ratio of the cross section of the pipe conveyor. The belt speed varied from 0,2 m/s to 10 m/s. The growth of the load of the pipe conveyor causes the decrease of the indentation factor. The reason of this effect is the influence of the presence of the forces from the stiffness of the belt material. In this case, according to the formula (29) for the low material loads, the numerator is larger than denominator, as it takes into account the forces caused by the stiffness of the belt material. For higher material loads, the stiffness forces stay the same, but impact of the material load increases, which in turn decreases the overall friction coefficient.

The dependence of the rolling friction coefficient for the pipe belt conveyor with 25% filling ratio and for the trough belt conveyor with the same load as for the pipe belt conveyor, is presented in Figure 9. The graphs, illustrated on Figure 9 show that the indentation rolling resistance friction factor for pipe belt conveyors is higher than for the open trough belt conveyor. The values for the indentation friction factor for the open trough belt conveyor were obtained as it was derived by May et al. in [8].
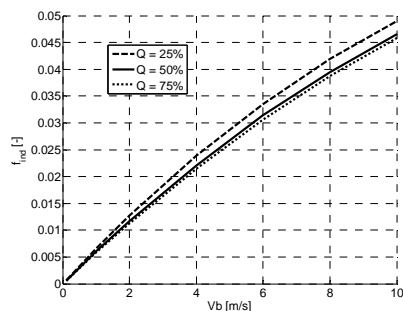
Figure 8. Influence of the percentage of the pipe conveyor load on the indentation rolling resistance factor versus speed.
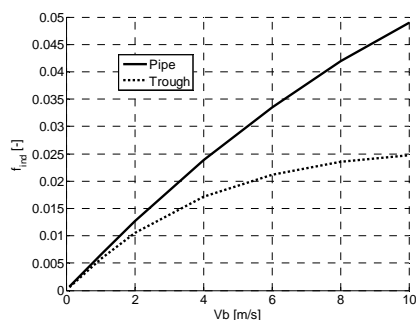

Figure 9. Indentation rolling resistance factor for pipe belt conveyor and for open trough belt conveyor versus speed.

5. CONCLUSION

A computational method has been constructed for the determination of the indentation rolling resistance for a pipe belt conveyor system. The presented model describes the calculation method for the load normal contact forces from the belt and material. The viscoelastic behaviour of the belt's rubber is modelled as a three-dimensional generalized model with multiple Maxwell parameters comprised with a Winkler foundation. The results were obtained for varied percentage load of the pipe conveyor. They show, that load increase causes decreased indentation rolling resistance factor. This phenomena is explained by the presence of the forces caused by the stiffness of the belt material. The simulation also demonstrate, that the indentation rolling resistance factor for pipe belt conveyors is higher in comparison with the conventional open trough belt conveyors. The viscoelastic Maxwell parameters were obtained from the rubber test, as a consequence, the model needs further extension, taking in account the complexity of the belt structure. Future research on the presented calculation method will be also focused on the correction normal forces from the stiffness of the belt and load from the material. The mathematical assumption for the calculation stiffness of the belt in this paper did not take in account the overlap geometry of the pipe. In presented formulas for the calculation of the material load needs to comprise some correction factors for high speed of the belt.

REFERENCES

[1] Hager, M. and Hintz, A.: The Energy-Saving Design of Belts for Long Conveyor Systems, Bulk Solids Handling, Vol. 13, pp. 749, 1993.

[2] Dmitriev, V.G. and Sergeeva, N.V.: Tension calculation of pipe belt conveyors, GIAB M, Moscow State Mining University, Vol. 16, pp. 144-170, 2009, (in Russian).

[3] Jonkers, C.O: The indentation rolling resistance of belt conveyors, Fordern und Heben, Vol. 30, pp. 312-316, 1980.

[4] Lodewijks, G.: Rolling resistance of conveyor belts, Bulk Solids Handling, Vol. 15, pp. 15-22, 1995.

[5] Gushin, V.M.: Determination parameters of the load-carrying surface for the steep inclined conveyors with the deep troughed belt, Mine and Quarry Transport, Nedra, Vol. 1, pp. 164-166, 1975, (in Russian).

[6] Chernenko, V.,D.: *Calculation of the continuous transportation systems*, Saint-Petersburg, Politehnika, 2008, (in Russian).

[7] Spaans, C.: Calculation of the main resistance of belt conveyors, Bulk Solids Handling, Vol. 11, pp. 809-820, 1991.

[8] May, W.D., Morris, E.L. and Atack, D.: Rolling friction of a hard cylinder over a viscoelastic material, Journal of Applied Physics, Vol. 30, No. 11, pp. 1713-1724, 1959.

[9] Hunter, S.C.: The rolling contact of a rigid cylinder with a viscoelastic half space, Journal of Applied Mechanics, Vol. 28, No. 4, pp. 611-617, 1961.

[10] Rudolphi, T.J. and Reicks, A.V.: Viscoelastic indentation and resistance to motion of conveyor belts using a generalized maxwell model of the backing material, Rubber Chemistry and Technology, Vol. 79, pp. 307-319, 2006.

[11] Nuttall, A.J.G., Lodewijks, G., and Klein Breteler, A.G., Modelling rolling contact phenomena in a pouch belt conveyor system, Wear, Vol. 260, No. 9-10, pp. 1081-1089, 2006.

ПОТРОШЊА ЕНЕРГИЈЕ ЦЕВНИХ ТРАКАСТИХ ТРАНСПОРТЕРА: ОТПОР КРЕТАЊУ ТРАКЕ ПРЕКО ВАЉАКА

Марија Е. Замиралова, Габријел Лодевајкс

Овај рад приказује детаљан приступ прорачуна сила отпора кретању траке преко ваљака цевних тракастих транспортера. Вискоеластично понашање гумене траке је моделирано као генерализовани тродимензионални модел са вишеструким Максвеловима параметрима на Винклеровом фундаменту. Постепени прорачун отпора кретању траке преко ваљака приказан је у раду. Посебна пажња је посвећена одређивању нормалних контактних сила као концентрисаних сила оптерећења на сваком ваљку у слогу ваљака. Оптерећење зависи од масе транспортованог материјала, степена испуњености цеви као и масе и крутости траке.